

## SEISMIC SOURCE PROPERTIES: INDICATIONS OF LITHOSPHERE IRREGULAR STRUCTURE ON DEPTH BENEATH VRANCEA REGION

E. Popescu, B. Grecu, M. Popa, M. Rizescu, M. Radulian

National Institute for Earth Physics, Bucharest-Magurele, PO.BOX MG-2

(Received July 15, 2003)

*Abstract.* The previous research focused on seismic regime properties in the Vrancea region (seismicity, tomography, seismic source scaling) revealed significant variation along the subducting slab. It has been assumed that this irregularity should be in connection with multiple parameter and multi-scale fields, and should reflect differences in the physical, geochemical and tectonic processes at different scale lengths. The recent development of the seismic network on the Romanian territory through the installation of digital accelerometers within the Collaborative Research Centre 461 Programme [5] and the tomography experiment CALIXTO'99 [24] has provided a substantial new amount of high-quality data in addition to the routine data coming from the Romanian seismic network (18 short-period, one-component instruments), dedicated firstly to seismicity monitoring. The main purpose of the present study is to incorporate this new data in the analysis of the depth dependence of the seismic source scaling in the Vrancea subducting slab. Spectral analysis and spectral ratios methods are applied for a set of 100 earthquakes with magnitudes  $2.9 \leq M_w \leq 5.3$ , occurred between 1996 and 2001. The two methods are employed independently, first to individual events, the second to pairs of collocated events and similar focal mechanism, in order to inspect the scaling properties over the seismic active depth domain (60-220 km). The results are discussed in connection with previous studies based on fractal statistics analysis. The clustering properties of time, space and size distributions as well as the scaling variations in the subducting lithosphere are ascribed to differences in specific source mechanisms or/and structural hierarchical inhomogeneity properties.

**Key words:** seismic source, lithosphere, fractal analysis, Vrancea region.

### INTRODUCTION

The seismicity and tomography studies on Vrancea seismic region suggest the presence of two seismic active segments along the subducting slab. An upper segment ( $60 \leq h \leq 110$  km), denoted with A in the following, and a lower segment ( $110 < h \leq 220$  km), denoted with C, are separated by a possible transition zone around 100 km depth, denoted with B. The active segments, A and C, differ as regards the seismicity rate and the total seismic energy release. They also differ in respect with the orientation angle of the subducted lithospheric blocks, which is changing around 90 - 110 km depth, in the B zone.

Significant differences along the subducting slab have been outlined by the studies focused on source properties analysis of Vrancea earthquakes (scaling, clustering and focal mechanism) as well [21], [22], [19], [2], [15], [18]. This depth variation was ascribed to specific mechanisms on different depth segments. For example, a dehydration reaction was assumed to be activated at around 100 km depth, similarly with what was noticed in other subduction regions and in agreement with new thermal-petrologic models of subduction zones. This would explain the differences in the fault plane solutions obtained for the transition zone as compared with the upper and lower active segments [14] and the particularities of clustering properties here.

The purpose of this paper is to extend the analysis of the depth dependence of the seismic source scaling in the Vrancea (Romania) subducting slab, using the new data coming from the CALIXTO'99 tomography experiment [24] and the network of digital accelerometers installed within CRC461 Programme [5]. Spectral analysis and spectral ratios methods are employed, first to individual events, the second to pairs of collocated events and similar focal mechanism, in order to inspect the scaling properties over the seismic active depth domain (60-220 km). The results are discussed in connection with previous studies based on fractal statistics analysis (variation coefficient, integral correlation methods). The clustering properties of time, space and size distributions as well as the scaling variations in the subducting lithosphere are ascribed to differences in specific source mechanisms or/and structural hierarchical inhomogeneity properties.

### Estimation of source parameters

#### *Spectral inversion method*

First we determine the source parameters (moment magnitude  $M_w$ , seismic moment  $M_o$ , seismic energy  $E_s$ , source radius  $r$ , stress drop  $\Delta\sigma$  and dislocation  $D$ ) using the SRCPLUS inversion algorithm [20] and [13]. This algorithm determines the seismic moment tensor from the inversion of the displacement waveforms

following the method of [9] and computes the source parameters by using several techniques [1], [3] on the basis of [7] model. The displacement spectra of the P and S body waves are computed for each station and are subsequently corrected for the effects of geometrical spreading, attenuation, seismic source pattern and free surface. In the hypothesis of Brune's  $\omega^2$  model, the average spectral parameters (low- and high-frequency asymptotes, corner frequency) are used to constrain the source parameters.

We consider a data set consisting of 81 intermediate-depth earthquakes ( $2.9 \leq M_w \leq 5.3$ ) recorded between 1996 and 2001 by the seismic network of K2 digital accelerometers installed within the German-Romanian cooperation (CRC461 Programme). The K2 network has an acceptable azimuthal coverage relative to Vrancea events and allows a high-quality processing of the waveforms in order to constrain the source parameters. The considered earthquakes are listed in *Table 1*.

*Table 1.* The considered earthquakes and the computed source parameters

No	Date	Time hh:mm	$\phi$ (°N)	$\lambda$ (°E)	h (km)	$M_w$	$M_0$ (Nm)	a (m)	D (cm)	$\Delta\sigma$ (MPa)
1	1996/01/30	04:36	45.73	26.66	102	4.3	$4.1 \times 10^{15}$	507	7	14
2	1996/06/07	05:09	45.52	26.32	126	4.6	$1.1 \times 10^{16}$	562	15	26
3	1996/12/12	03:30	45.65	26.48	133	3.6	$2.3 \times 10^{14}$	368	1	3
4	1997/01/01	01:44	45.79	26.62	148	3.8	$7.3 \times 10^{14}$	268	4	17
5	1997/03/01	19:26	45.71	26.63	104	4.2	$2.5 \times 10^{15}$	286	13	48
6	1997/05/31	05:29	45.66	26.41	127	3.7	$4.9 \times 10^{14}$	285	3	9
7	1997/07/14	00:37	45.77	26.75	128	4.2	$2.9 \times 10^{15}$	221	25	117
8	1997/08/24	09:18	45.71	26.54	136	3.9	$8.3 \times 10^{14}$	218	7	35
9	1997/10/11	19:00	45.80	26.80	110	4.5	$7.9 \times 10^{15}$	397	22	55
10	1997/10/22	07:49	45.59	26.39	134	4.0	$1.2 \times 10^{15}$	372	3	10
11	1997/11/18	11:23	45.76	26.71	123	4.7	$1.3 \times 10^{16}$	411	34	84
12	1997/12/18	23:21	45.52	26.26	136	3.9	$9.9 \times 10^{14}$	342	3	11
13	1997/12/30	04:39	45.54	26.32	139	4.6	$9.3 \times 10^{15}$	401	23	63
14	1998/01/14	05:01	45.71	26.60	143	4.0	$1.1 \times 10^{15}$	321	4	15
15	1998/01/19	00:53	45.64	26.67	105	4.0	$1.5 \times 10^{15}$	302	7	21
16	1998/01/31	21:14	45.47	26.33	137	3.6	$3.4 \times 10^{14}$	230	3	12
17	1998/02/19	14:34	45.84	26.70	140	3.8	$7.4 \times 10^{14}$	369	2	6
18	1998/03/13	13:14	45.56	26.33	155	4.7	$1.4 \times 10^{16}$	474	25	57
19	1998/04/14	01:03	45.73	26.57	141	3.8	$7.3 \times 10^{14}$	293	3	13
20	1998/04/23	06:37	45.81	26.64	97	3.5	$2.4 \times 10^{14}$	261	2	6
21	1998/05/04	16:10	45.73	26.45	145	4.0	$1.1 \times 10^{15}$	331	4	13
22	1998/06/02	04:48	45.65	26.40	115	3.4	$1.1 \times 10^{14}$	335	1	2
23	1998/06/06	20:34	45.67	26.53	149	3.0	$3.8 \times 10^{13}$	450	0.1	0.2
24	1998/07/03	06:14	45.68	26.76	136	4.2	$2.1 \times 10^{15}$	298	10	35
25	1998/07/27	15:02	45.67	26.53	135	4.4	$4.5 \times 10^{15}$	389	2	33
26	1998/08/24	23:27	45.71	26.45	165	3.6	$3.2 \times 10^{14}$	293	2	5
27	1998/09/21	13:49	45.80	26.62	148	3.6	$3.2 \times 10^{14}$	276	2	7
28	1998/11/14	11:15	45.76	26.58	146	3.6	$3.0 \times 10^{14}$	228	2	1
29	1998/12/12	10:55	45.51	26.26	150	3.4	$1.8 \times 10^{14}$	440	0.4	1
30	1998/12/17	19:15	45.80	26.68	136	3.2	$7.9 \times 10^{13}$	215	1	3
31	1998/12/28	21:50	45.78	26.47	157	2.9	$2.8 \times 10^{13}$	215	0.2	1
32	1998/12/29	05:56	45.61	26.52	118	3.7	$4.1 \times 10^{14}$	234	3	14
33	1999/01/06	21:28	45.54	26.28	121	3.1	$6.4 \times 10^{13}$	271	0.4	1
34	1999/01/09	00:04	45.54	26.38	146	3.1	$5.3 \times 10^{13}$	256	0.3	1
35	1999/01/23	17:01	45.67	26.48	140	4.1	$1.9 \times 10^{15}$	442	4	10
36	1999/02/22	10:01	45.66	26.51	127	3.3	$1.2 \times 10^{14}$	268	1	3
37	1999/03/09	17:51	45.66	26.47	151	3.4	$1.7 \times 10^{14}$	336	1	3
38	1999/03/17	07:01	45.62	26.46	158	3.4	$1.6 \times 10^{14}$	229	1	6
39	1999/03/17	22:10	45.70	26.56	142	4.1	$1.6 \times 10^{15}$	359	5	15
40	1999/03/22	19:25	45.52	26.31	145	4.4	$4.7 \times 10^{15}$	415	11	29
41	1999/03/23	09:11	45.68	26.50	155	4.0	$1.2 \times 10^{15}$	270	7	27
42	1999/04/04	01:21	45.70	26.45	146	3.7	$4.2 \times 10^{14}$	225	3	16
43	1999/04/15	02:21	45.87	26.80	89	3.3	$1.2 \times 10^{14}$	236	1	4

## Seismic source properties

44	1999/04/28	08:47	45.49	26.27	151	5.3	$1.3 \times 10^{17}$	677	111	177
45	1999/04/29	18:44	45.62	26.40	148	4.0	$1.4 \times 10^{15}$	306	6	21
46	1999/04/30	22:32	45.53	26.24	148	3.2	$7.4 \times 10^{13}$	214	1	3
47	1999/05/25	09:35	45.59	26.49	122	3.9	$8.9 \times 10^{14}$	272	5	19
48	1999/06/11	08:20	45.84	26.63	112	3.3	$1.2 \times 10^{14}$	267	1	3
49	1999/06/20	00:09	45.60	26.52	131	3.6	$2.9 \times 10^{14}$	224	2	4
50	1999/06/22	08:02	45.72	26.46	149	3.7	$5.1 \times 10^{14}$	233	4	18
51	1999/06/29	20:04	45.61	26.52	131	4.2	$3.0 \times 10^{15}$	407	7	19
52	1999/07/04	08:21	45.41	26.21	149	3.3	$1.2 \times 10^{14}$	223	1	5
53	1999/07/13	13:10	45.70	26.49	132	4.0	$1.1 \times 10^{15}$	308	5	16
54	1999/07/15	02:52	45.84	26.77	113	3.0	$3.6 \times 10^{13}$	226	0.3	1
55	1999/08/07	02:25	45.67	26.43	133	3.7	$3.8 \times 10^{14}$	344	1	4
56	1999/09/14	23:48	45.61	26.51	124	3.1	$5.5 \times 10^{13}$	271	0.3	1
57	1999/10/12	23:48	45.71	26.39	164	3.7	$3.9 \times 10^{14}$	225	3	15
58	1999/11/08	19:22	45.55	26.35	138	4.6	$1.1 \times 10^{16}$	414	26	67
59	1999/11/14	09:05	45.52	26.27	132	4.6	$1.0 \times 10^{16}$	515	16	33
60	1999/11/24	03:57	45.85	26.76	112	3.4	$1.8 \times 10^{14}$	246	1	5
61	1999/12/17	16:06	45.80	26.66	82	3.4	$1.9 \times 10^{14}$	233	2	6
62	2000/03/08	22:11	45.87	26.71	71	4.1	$1.8 \times 10^{15}$	547	3	5
63	2000/04/06	00:10	45.76	26.65	147	4.8	$2.2 \times 10^{16}$	664	20	33
64	2000/05/10	04:27	45.61	26.55	131	4.0	$1.4 \times 10^{15}$	344	5	16
65	2000/07/01	20:50	45.81	26.80	64	3.6	$3.6 \times 10^{14}$	306	2	6
66	2000/07/15	08:42	45.75	26.55	144	3.4	$1.5 \times 10^{14}$	356	1	2
67	2000/07/27	02:39	45.87	26.68	138	3.4	$1.6 \times 10^{14}$	278	1	3
68	2000/08/06	05:09	45.62	26.24	161	3.2	$8.6 \times 10^{13}$	318	0.3	1
69	2000/08/10	19:58	45.64	26.39	130	3.5	$2.1 \times 10^{14}$	350	1	2
70	2000/10/12	08:42	45.77	26.50	149	3.5	$2.1 \times 10^{14}$	235	2	7
71	2000/11/30	21:31	45.69	26.47	144	3.7	$4.1 \times 10^{14}$	613	0.5	1
72	2000/12/16	12:47	45.79	26.57	155	4.2	$2.4 \times 10^{15}$	309	10	36
73	2001/03/04	15:38	45.52	26.23	156	4.5	$8.0 \times 10^{15}$	533	11	23
74	2001/03/18	06:33	45.52	26.22	153	3.6	$3.6 \times 10^{14}$	324	1	5
75	2001/03/28	22:07	45.76	26.67	133	3.9	$8.2 \times 10^{14}$	279	4	16
76	2001/05/20	03:59	45.61	26.44	153	3.8	$7.0 \times 10^{14}$	226	6	27
77	2001/05/24	17:34	45.66	26.49	156	5.0	$4.1 \times 10^{16}$	623	43	75
78	2001/07/20	05:09	45.78	26.74	128	4.9	$2.4 \times 10^{16}$	478	46	97
79	2001/08/02	04:48	45.74	26.55	133	4.0	$1.1 \times 10^{15}$	267	6	25
80	2001/10/17	13:01	45.66	26.51	98	4.5	$7.0 \times 10^{15}$	357	25	67
81	2001/10/17	15:35	45.74	26.47	158	3.4	$4.6 \times 10^{14}$	245	3	14

The spectrum of the displacement field in the far field is given by:

$$\Omega_s(\omega) = R(\Delta\sigma/\mu)\beta(a/r)\{1/[\omega^2 + (2.34\beta/a)^2]\} \quad (1)$$

where  $r$  is the distance source-station,  $\beta$  is the S-wave propagation velocity,  $R$  is the radiation pattern,  $\mu$  is the rigidity modulus of the medium,  $a$  is the source dimension,  $\omega = 2\pi f$  ( $f$  – frequency).  $\Delta\sigma$  is effective stress drop or dynamic stress drop and represents the difference between the initial stress on fault and the final frictional stress which resists to the fault slip. Asymptotically, the spectrum tends to the constant value

$$\Omega_o = \Omega_s(\omega \rightarrow 0) = (R/4\pi r \beta^3)M_o = M_o/F \quad (2)$$

which is proportional to the seismic moment  $M_o$  (the proportionality factor  $F$  depends on the radiation pattern, geometrical spreading and seismic wave velocity). Relation (2) is valid both in case of S and P waves with the corresponding seismic wave velocity and radiation pattern in equation (2).

According to (1), the displacement spectrum decreases as  $\omega^{-2}$  for frequencies greater than the corner frequency  $f_c$ , which is given by the intersection of the low-frequency asymptote and the high-frequency asymptote (Fig. 1). Typically the corner frequency is related to a characteristic dimension of the source. For a circular source, the corner frequency is inversely proportional to the fault radius [7]:

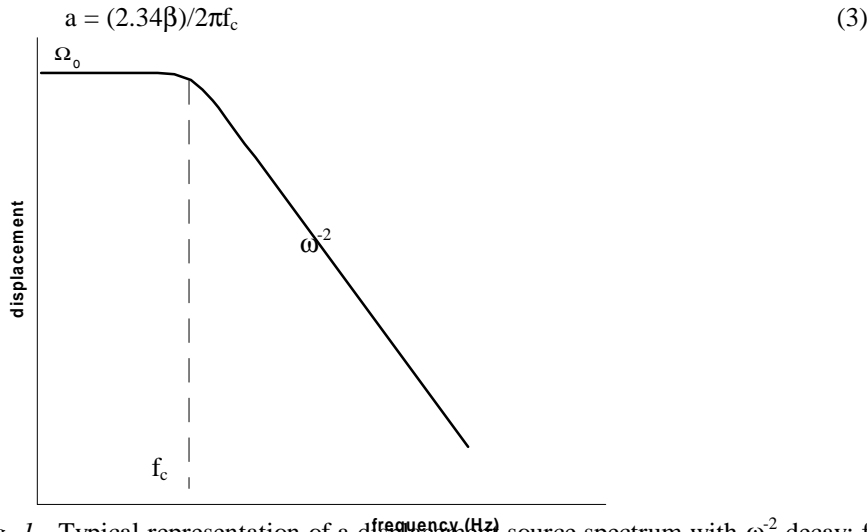


Fig. 1. -Typical representation of a displacement source spectrum with  $\omega^{-2}$  decay;  $f_c$  is the corner frequency;  $\Omega_0$  is the low-frequency level.

Equation (1) is deduced assuming that the entire stress accumulated on fault is released during the earthquake, so that the stress drop  $\Delta\sigma$  is defined as the difference between the final and initial stresses averaged over the fault plane. In these conditions the seismic moment and the stress drop are related through the following relation:

$$\Delta\sigma = (7/16)(M_o/a^3) \quad (4)$$

The magnitude  $M_W$  is estimated from seismic moment by:

$$M_W = (\log M_o - 9.1)/1.5 \quad (5)$$

The seismic moment  $M_o$  is estimated for each station using (1) after correcting the displacement spectra for geometrical spreading, radiation pattern and free surface response. Finally, a mean value is adopted for the all available stations. The radius  $a$  and the stress drop  $\Delta\sigma$  are evaluated using (3), and (4), respectively. The dislocation on fault  $D$  is determined by:

$$D = M_o/(\mu\pi a^2) \quad (6)$$

The resulted parameters are given in *Table 1*.

#### *Spectral ratio method*

The spectral ratios for two earthquakes with foci located close one another mainly reflect the source properties, while the path effects are to a large extent eliminated. For a source model with homogeneous rupture and high-frequency fall-off  $\omega^{-\gamma}$ , the spectral ratio  $R(f)$  can be approximated by the theoretical function:

$$R(f) = \frac{\Omega_0^p [1 + (f/f_c^s)^{2\gamma}]^{1/2}}{\Omega_0^s [1 + (f/f_c^p)^{2\gamma}]^{1/2}} \quad (7)$$

where  $f_c^p$  and  $f_c^s$  are the corner frequencies of the main event and Green's event, respectively, and  $\Omega_0^p$  and  $\Omega_0^s$  are the low-frequency spectral levels. For a better constraint of the corner frequencies and spectral levels it is necessary to use broadband recordings [11]. In the following, we applied the spectral ratio method for the broadband seismograms recorded at Vrâncioaia (VRI) seismic station, located in the epicentral area, for 37 earthquakes (*Table 2*). Only P waves were considered.

*Table 2.* List of the earthquakes considered in spectral ratios analysis. The main events are marked by bold characters. One or more co-located events are associated with each main event

## Seismic source properties

No.	Data	hour:min	lat. (°N)	Lon. (°E)	H (km)	M <sub>w</sub>	M <sub>D</sub>
<b>1</b>	<b>1997/03/01</b>	<b>19:26</b>	<b>45.71</b>	<b>26.63</b>	<b>104</b>	<b>4.2</b>	<b>4.4</b>
2	1997/12/17	02:48	45.73	26.69	77	-	3.1
3	1998/12/01	02:38	45.74	26.65	76	-	3.6
4	1999/07/03	15:21	45.79	26.82	92	-	3.4
5	1999/09/04	00:26	45.71	26.68	70	-	3.1
6	1999/10/12	19:23	45.70	26.61	83	-	3.4
7	1999/11/09	02:09	45.71	26.61	92	-	3.4
<b>8</b>	<b>1998/01/19</b>	<b>00:53</b>	<b>45.64</b>	<b>26.67</b>	<b>105</b>	<b>4.0</b>	<b>4.7</b>
9	1998/07/02	20:50	45.71	26.67	108	-	3.9
10	1999/01/18	21:35	45.60	26.66	118	-	3.6
11	1999/11/09	02:09	45.71	26.61	92	-	3.4
<b>12</b>	<b>1999/04/28</b>	<b>08:47</b>	<b>45.49</b>	<b>26.27</b>	<b>151</b>	<b>5.3</b>	<b>6.2</b>
13	1998/12/12	10:55	45.51	26.26	150	3.4	4.2
14	1999/01/06	21:28	45.54	26.28	121	3.1	4.0
15	1999/04/30	22:32	45.53	26.16	148	3.2	4.3
16	1999/06/06	12:01	45.53	26.32	136	-	3.9
17	1999/11/08	19:22	45.55	26.35	138	4.6	5.2
18	1999/11/14	09:05	45.52	26.27	132	4.6	5.2
19	2000/03/28	06:40	45.48	26.32	137	-	3.7
<b>20</b>	<b>2000/03/08</b>	<b>22:11</b>	<b>45.87</b>	<b>26.71</b>	<b>71</b>	<b>4.1</b>	<b>5.2</b>
21	1997/07/04	00:30	45.80	26.85	77	-	3.7
<b>22</b>	<b>2000/04/06</b>	<b>00:10</b>	<b>45.76</b>	<b>26.65</b>	<b>147</b>	<b>4.8</b>	<b>5.4</b>
23	1998/09/21	13:49	45.80	26.62	148	3.6	4.5
24	1998/09/22	20:52	45.74	26.60	142	-	3.7
25	1998/11/14	11:15	45.76	26.58	146	3.6	4.4
26	1999/05/05	16:21	45.67	26.56	142	-	4.1
27	1999/08/09	07:17	45.73	26.70	133	-	4.2
28	1999/08/28	05:32	45.70	26.63	142	-	4.0
<b>29</b>	<b>1996/06/07</b>	<b>05:09</b>	<b>45.52</b>	<b>26.32</b>	<b>128</b>	<b>4.6</b>	<b>5.4</b>
16	1999/06/06	12:01	45.51	26.32	136	-	3.9
<b>30</b>	<b>1997/10/11</b>	<b>19:00</b>	<b>45.80</b>	<b>26.80</b>	<b>110</b>	<b>4.5</b>	<b>5.5</b>
31	1996/02/03	07:07	45.79	26.84	100	-	4.3
32	1999/04/15	02:21	45.87	26.80	89	3.3	4.0
33	1999/05/17	16:33	45.79	26.79	110	-	3.8
<b>34</b>	<b>1997/11/18</b>	<b>11:23</b>	<b>45.76</b>	<b>26.71</b>	<b>123</b>	<b>4.7</b>	<b>5.5</b>
35	1999/07/14	13:27	45.68	26.59	148	-	4.0
23	1998/09/21	13:49	45.80	26.62	148	3.6	4.5
25	1998/11/14	11:15	45.76	26.58	146	3.6	4.4
27	1999/08/09	07:16	45.73	26.70	133	-	4.2
<b>36</b>	<b>1998/03/13</b>	<b>13:14</b>	<b>45.56</b>	<b>26.33</b>	<b>155</b>	<b>4.7</b>	<b>5.5</b>
37	1996/10/15	04:43	45.51	26.38	152	-	4.2
15	1999/04/30	22:32	45.53	26.24	148	3.2	4.3

The source parameters obtained by spectral ratios analysis are given in *Table 3*.

*Table 3.* Source parameters estimated by spectral ratios method

No.	M <sub>0</sub> (Nm)	f <sub>c</sub> <sup>a</sup> (Hz)	f <sub>c</sub> <sup>b</sup> (Hz)	a (m)	Δσ (MPa)	f <sub>max</sub> (Hz)	m
<b>1</b>	<b>2.50 x 10<sup>15</sup></b>	<b>5.2</b>	<b>4.3</b>	<b>418</b>	<b>15</b>	<b>10.4</b>	<b>2.4</b>
2	4.57 x 10 <sup>13</sup>	14.5	15.6	115	15	17.5	3.8
3	2.24 x 10 <sup>13</sup>	12.8	12.2	148	3	15.3	3.1
4	7.08 x 10 <sup>13</sup>	10.1	12.1	149	9	14.2	2.8
5	4.17 x 10 <sup>13</sup>	12.6	13.4	134	8	13.0	3.0

6	$4.26 \times 10^{13}$	9.2	12.7	142	7	11.5	2.5
7	$3.71 \times 10^{13}$	10.7	11.2	160	4	12.0	3.8
<b>8</b>	<b><math>1.50 \times 10^{15}</math></b>	<b>3.4</b>	<b>3.5</b>	<b>518</b>	<b>5</b>	<b>15.5</b>	<b>3.7</b>
9	$2.24 \times 10^{14}$	11.1	10.3	176	18	13.1	2.7
10	$1.50 \times 10^{13}$	6.2	7.3	250	0.4	14.2	3.1
11	$1.68 \times 10^{13}$	7.7	9.3	195	1	17.1	3.8
<b>12</b>	<b><math>1.30 \times 10^{17}</math></b>	<b>1.6</b>	<b>1.8</b>	<b>990</b>	<b>59</b>	<b>12.4</b>	<b>3.2</b>
13	$6.70 \times 10^{12}$	4.00	7.4	255	0.2	8.0	3.0
14	$7.63 \times 10^{13}$	7.9	6.8	284	2	11.8	3.6
15	$7.01 \times 10^{13}$	6.9	7.1	269	2	13.6	3.3
16	$1.99 \times 10^{13}$	8.3	8.4	237	0.7	14.8	3.4
17	$8.61 \times 10^{15}$	1.9	2.1	925	5	6.4	2.6*
18	$1.14 \times 10^{16}$	2.3	1.7	1083	4	6.2	2.3
19	$5.97 \times 10^{12}$	8.0	7.6	247	0.2	10	3.0
<b>20</b>	<b><math>7.08 \times 10^{16}</math></b>	<b>4.4</b>	<b>3.6</b>	<b>505</b>	<b>241</b>	<b>8.9</b>	<b>3.5*</b>
21	$2.24 \times 10^{15}$	7.2	8.1	153	90	8.9	3.7
<b>22</b>	<b><math>3.90 \times 10^{16}</math></b>	<b>2.1</b>	<b>1.9</b>	<b>995</b>	<b>17</b>	<b>7.4</b>	<b>2.7</b>
23	$1.26 \times 10^{14}$	5.1	6.8	273	3	10.6	2.8
24	$1.21 \times 10^{13}$	6.9	17.9	104	5	13.8	3.4
25	$1.83 \times 10^{14}$	5.9	7.9	235	6	9.2	2.8
26	$4.88 \times 10^{13}$	6.9	8.9	207	2	10.1	3.1
27	$6.92 \times 10^{13}$	5.4	8.4	226	3	9.1	3.5
28	$6.77 \times 10^{13}$	7.0	9.6	193	4	11.6	2.4
<b>29</b>	<b><math>1.10 \times 10^{16}</math></b>	<b>5.4</b>	<b>3.22</b>	<b>575</b>	<b>25</b>	<b>14.28</b>	<b>2.4</b>
16	$2.45 \times 10^{13}$	9.43	7.87	235	0.8	16.53	2.1
<b>30</b>	<b><math>7.90 \times 10^{15}</math></b>	<b>2.57</b>	<b>1.93</b>	<b>940</b>	<b>4</b>	<b>17.41</b>	<b>3.3</b>
31	$4.99 \times 10^{114}$	7.50	6.96	260	12	15.15	2.8
32	$3.14 \times 10^{14}$	7.27	6.0	302	5	15.31	2.9
33	$1.30 \times 10^{14}$	6.85	7.5	243	4	17.00	3.1
<b>34</b>	<b><math>1.30 \times 10^{16}</math></b>	<b>2.75</b>	<b>1.92</b>	<b>964</b>	<b>6</b>	<b>14.80</b>	<b>3.3</b>
35	$9.64 \times 10^{14}$	4.59	3.1	597	2	10.20	3.3
23	$8.99 \times 10^{13}$	6.88	4.86	381	0.7	10.82	3.0
25	$1.67 \times 10^{14}$	5.0	4.89	250	1	16.58	2.6
27	$8.20 \times 10^{13}$	7.46	5.83	317	1	8.44	2.2
<b>36</b>	<b><math>1.40 \times 10^{16}</math></b>	<b>2.43</b>	<b>2.64</b>	<b>712</b>	<b>17</b>	<b>13.08</b>	<b>3.1</b>
37	$5.70 \times 10^{13}$	12.45	13.00	145	8	14.69	3.6
15	$8.83 \times 10^{13}$	7.47	8.68	216	3	17.91	3.6

\* parameter m was fixed in the regression

There are two estimations of the corner frequency: directly from the acceleration spectra ( $f_c^a$ ) and from the spectral ratios ( $f_c^b$ ) (the procedure for the corner frequency determination is presented in [18]). They generally correlate (one exception is for event 24) with a standard deviation of 1.45, as can be seen in Fig. 2 (where the outlier for the event 24 was removed). The source radius in Table 3 is computed using (3) and the corner frequency estimated from spectral ratios analysis. The maximum frequency of the acceleration spectrum,  $f_{max}$ , and the high-frequency slope,  $m$ , are estimated from the acceleration spectra.

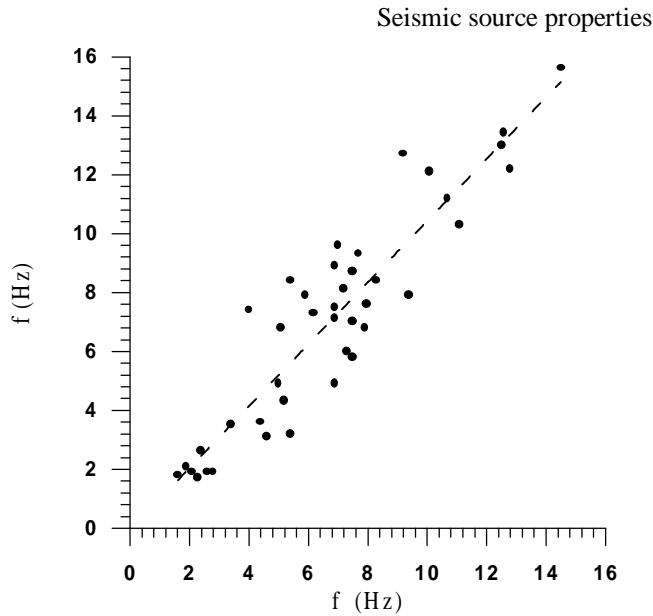


Fig 2.- Corner frequency obtained from spectral ratios versus corner frequency obtained from acceleration spectra

The comparison of the source radius resulted from spectra inversion and from spectral ratios (*Fig. 3*) shows significant greater values when using spectral ratios method. This could be due to fact that the spectra inversion is not correcting all the factors which distort the signal from the source (and first of all the site effects).

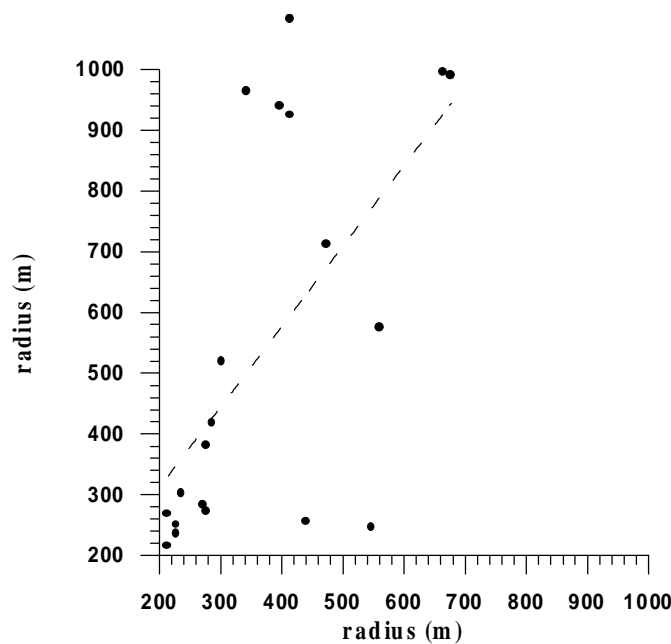


Fig 3.- Source radius determined by spectral ratios versus source radius determined by spectral inversion

### Source scaling

On the basis of the source parameters obtained in the previous section we evaluate the characteristic scaling relations of the Vrancea seismic source and look for possible depth dependency. We use separately the source parameter values obtained by inversion of spectra and spectral ratios method.

#### *Seismic moment-magnitude relation*

The magnitude is estimated from the recording duration. The seismic moment values (in Nm) vs. magnitude values obtained with spectral analysis method and spectral ratio method respectively are close each other, as can be seen in *Fig. 4.*, with a greater dispersion in the second case. The regression lines are:

$$\begin{aligned} \lg M_o &= (1.4 \pm 0.1) M_D + (8.6 \pm 0.4) \\ R &= 0.89, \sigma = 0.37 \end{aligned} \tag{8}$$

for spectral inversion, and

$$\begin{aligned} \lg M_o &= (1.3 \pm 0.1) M_D + (8.8 \pm 0.6) \\ R &= 0.86, \sigma = 0.64 \end{aligned} \tag{9}$$

for spectral ratio method.

*Moment magnitude - duration magnitude relation* is represented in Fig. 5. The corresponding regression line is:

$$\begin{aligned} M_W &= (0.9 \pm 0.0) M_D - (0.4 \pm 0.1) \\ R &= 0.79, \sigma = 0.06 \end{aligned} \tag{10}$$

for the values obtained by spectra inversion.

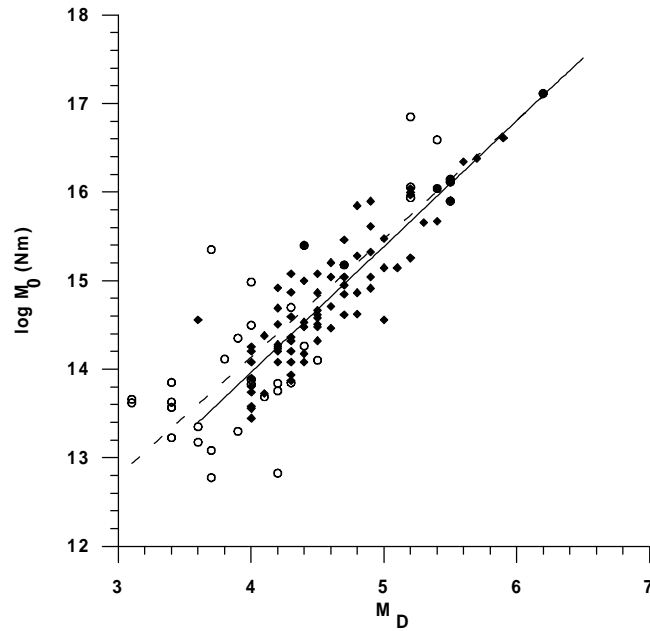


Fig. 4.- Seismic moment – duration magnitude relation. Solid circles – values obtained by spectral inversion; empty circles – values obtained by spectral ratios method.

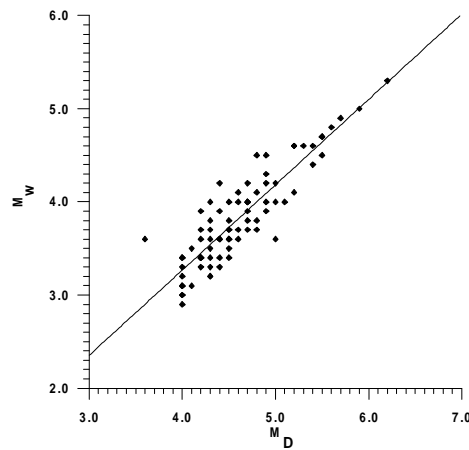


Fig. 5. -  $M_W$ -  $M_D$  relation: diamonds and solid line for spectral inversion.

*Seismic moment – source radius relation*

The following relations are obtained for the two sets of source parameters:  
Spectra inversion:

$$\lg M_0 = (4.0 \pm 0.5) \lg a + (4.8 \pm 1.2) \quad (11)$$

$$R = 0.68, \sigma = 0.57$$

Spectral ratios:

$$\lg M_0 = (3.4 \pm 0.4) \lg a + (6.2 \pm 0.9) \quad (12)$$

$$R = 0.83, \sigma = 0.68$$

where  $a$  is measured in meters. The regression lines are represented in *Fig. 6*. Again the dispersion is more pronounced for the values obtained by spectral ratios procedure. Both relations suggest a deviation from a source model with constant stress drop (characterized by a -3 slope), but this could be caused by errors as well.

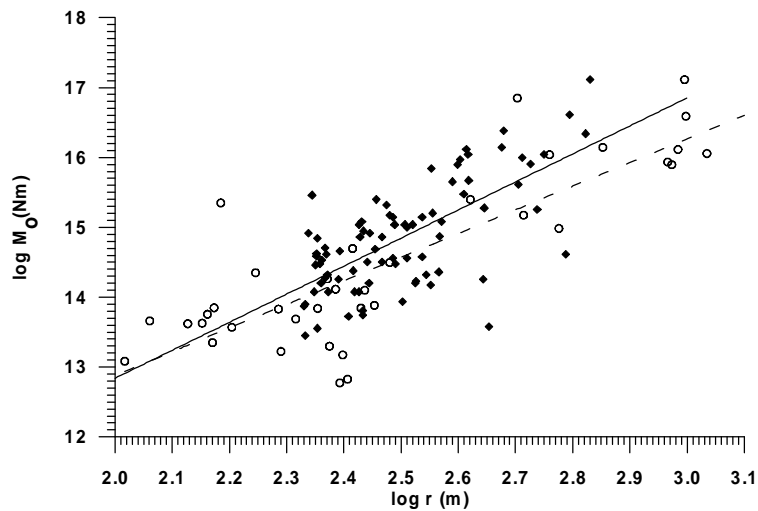


*Fig. 6.* - Seismic moment versus source radius for the entire depth domain: diamonds and solid line for spectral inversion and empty circles and dashed line for spectral ratios.

*Stress drop - seismic moment relation*

With stress drop values in MPa and seismic moment values in Nm, the following relations are obtained (*Fig. 7*):

Spectra inversion:

$$\lg \Delta\sigma = (0.7 \pm 0.0) \lg M_0 - (9.3 \pm 0.6) \quad (13)$$

$$R = 0.88, \sigma = 0.30$$

Spectral ratios:

$$\lg \Delta\sigma = (0.4 \pm 0.1) \lg M_0 - (4.5 \pm 0.9) \quad (14)$$

$$R = 0.69, \sigma = 0.47$$

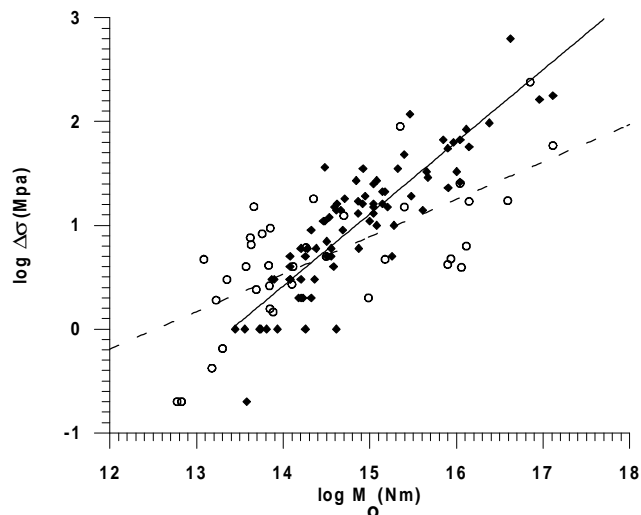


Fig. 7.- Stress drop-seismic moment dependence: diamonds and solid line for spectral inversion and empty circles and dashed line for spectral ratios.

The two relations show a deviation from a constant stress drop model, an increase of the stress drop with increasing seismic moment, respectively. This kind of scaling characterizes the complex source processes and seems to be quite common in case of Vrancea earthquakes [15].

*Seismic energy - seismic moment relation* is deduced only using the spectra inversion and is given by (Fig. 8):

$$\lg E_s = (1.7 \pm 0.1) \lg M_0 - (16.0 \pm 1.0) \quad (15)$$

$R=0.93, \sigma =0.52$

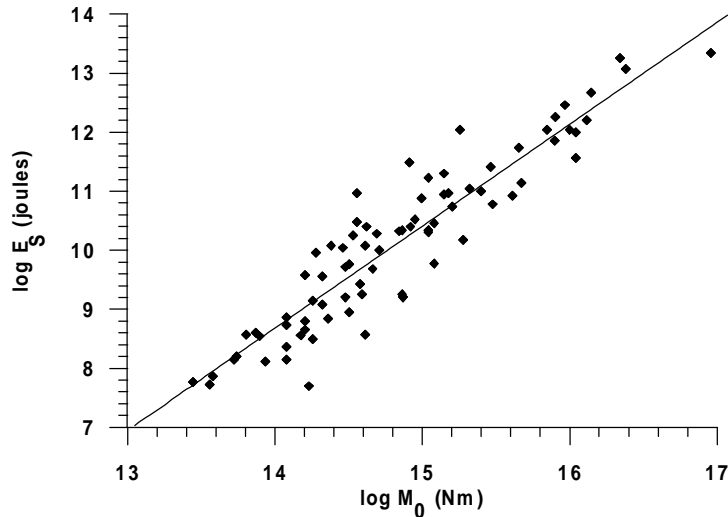


Fig. 8. - Seismic energy versus seismic moment: diamonds and solid line for spectral inversion.

Note that log Es~log M0 relation for the entire zone is dominated by data located in the lower segment of the subducting slab.

*Dislocation - seismic moment relation* was obtained also only for the spectra inversion case. For the dislocation given in cm, and seismic moment in Nm, the regression line is (Fig. 9):

$$\lg D = (0.7 \pm 0.0) \lg M_0 - (10.0 \pm 0.5) \quad (16)$$

$R=0.95, \sigma = 0.17$

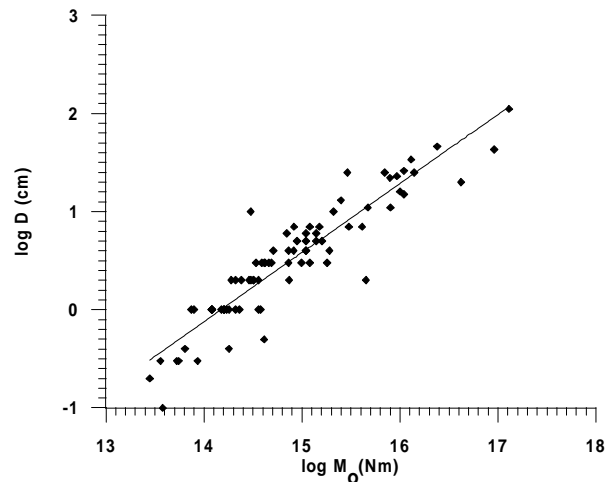
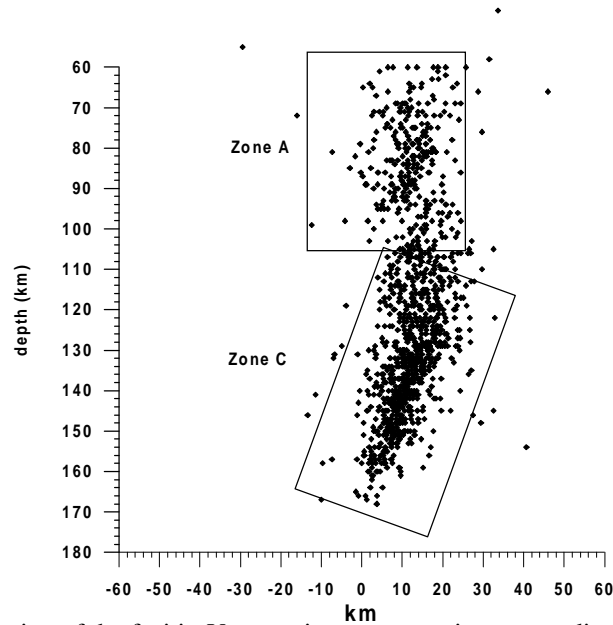


Fig. 9.- Dislocation-seismic moment dependence: diamonds and solid line for spectral inversion

### Depth variation of the scaling properties

There is an increasing number of evidence in favor of clustering in time, space and energy of the seismic process in Vrancea subcrustal domain, reflecting specific physical, geodynamical and rheological phenomena acting at different scale lengths at these depths. At the same time, the clustering is related to a hierarchical structure of the inhomogeneities that control the seismogenic process. At the scale of the entire subducting lithosphere, we can assume two [22] or even three active segments [10], [12], [17]. In the following we shall adopt the model of two seismogenic areas, A ( $60 \leq h \leq 110$  km) and C ( $110 < h \leq 220$  km) (**Fig. 10**), and analyze the scaling properties separately for the two zones in order to outline eventually depth-dependent variation. It is likely that the two active zones are separated by a sort of transition zone around 100 km depth.



**Fig. 10.** - Depth distribution of the foci in Vrancea in a cross section perpendicular to the Carpathians Arc. Two possible active segments are highlighted.

**The seismic moment – magnitude relations** for the two zones are (**Fig. 11**):

Zone A

*Spectral inversion*

$$\lg M_o = (1.2 \pm 0.3) M_D + (9.6 \pm 1.3) \quad (17)$$

$$R = 0.74, \sigma = 0.47$$

*Spectral ratios*

$$\lg M_o = (1.3 \pm 0.2) M_D + (9.3 \pm 0.8) \quad (18)$$

$$R = 0.87, \sigma = 0.53$$

Zone C

*Spectral inversion*

$$\lg M_o = (1.4 \pm 0.1) M_D + (8.2 \pm 0.4) \quad (19)$$

$$R = 0.92, \sigma = 0.32$$

*Spectral ratios*

$$\lg M_o = (1.8 \pm 0.2) M_D + (6.6 \pm 0.7) \quad (20)$$

$$R = 0.94, \sigma = 0.49$$

The correlation coefficient is greater and the errors are smaller for the deeper zone (C). Both methods indicate a slope of the seismic moment - magnitude relation that increases significantly on depth, in agreement with a substantial change in the earthquake generation process pointed out in the lower part of the subducting lithosphere relative to the upper part [22], [16].

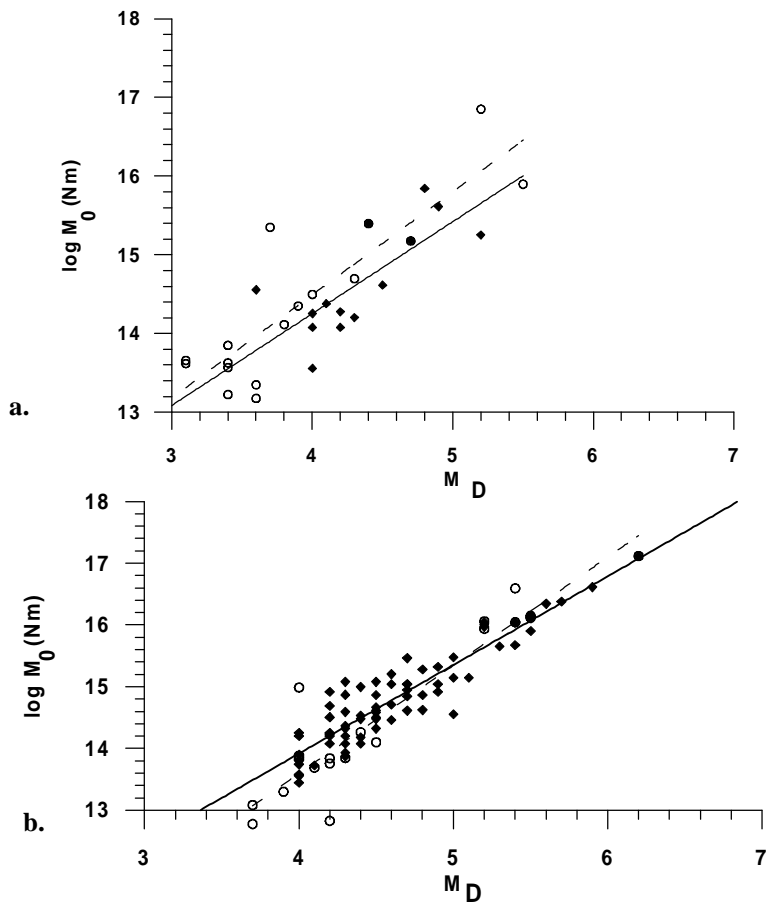


Fig. 11.- Seismic moment - magnitude relation: diamonds and solid line for spectral inversion and empty circles and dashed line for spectral ratios  
 a. zone A;  
 b. zone C.

*The seismic moment – source radius* dependences are approximated by the regression lines (Fig. 12):

Zone A

*Spectral inversion*

$$\lg M_0 = (3.9 \pm 1.2) \lg a + (5.0 \pm 2.8) \quad (21)$$

$$R = 0.70, \sigma = 0.50$$

*Spectral ratios*

$$\lg M_0 = (3.1 \pm 0.7) \lg a + (7.1 \pm 1.7) \quad (22)$$

$$R = 0.75, \sigma = 0.72$$

Zone C

*Spectral inversion*

$$\lg M_0 = (4.1 \pm 0.4) \lg a + (4.8 \pm 4.1) \quad (23)$$

$$R = 0.67, \sigma = 0.60$$

*Spectral ratios*

$$\lg M_0 = (4.1 \pm 0.4) \lg a + (4.1 \pm 1.1) \quad (24)$$

$$R = 0.92, \sigma = 0.55$$

## Seismic source properties

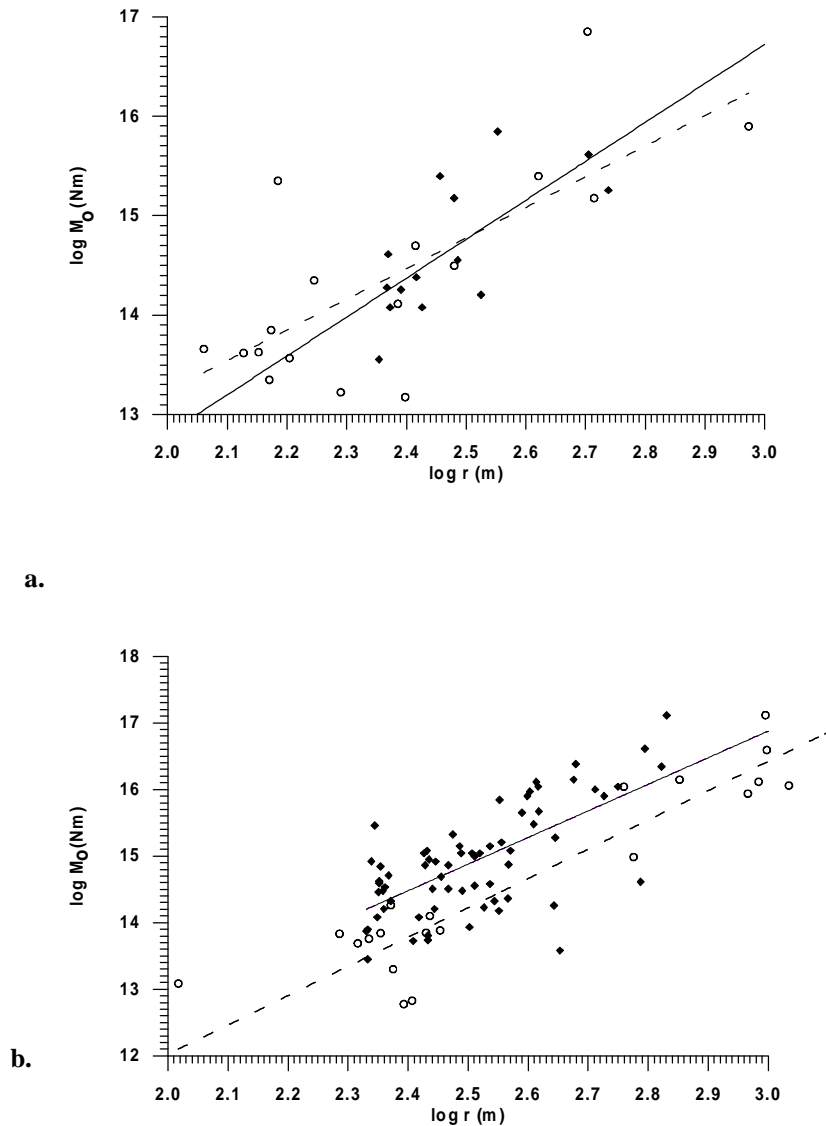


Fig. 12.- Seismic moment – source radius relation: diamonds and solid line for spectral inversion and empty circles and dashed line for spectral ratios

- a. zone A;  
b. zone C.

Except the relation obtained for zone A using spectral ratios method (slope  $\sim 3$ ), for all the other computations the slope of the seismic moment – source radius relation is close to 4, indicating a complex rupture process, especially in the lower lithosphere. This result agrees with the complex source time function retrieved by empirical Green's function deconvolution for the largest shock generated after 1990 in the zone C (28 April 1999,  $M_w=5.3$ ).

The relations between the stress drop and seismic moment are plotted in Fig. 13 and the regression approximations are:

Zone A:

*Spectral inversion*

$$\lg \Delta\sigma = (0.7 \pm 0.1) \lg M_0 - (8.6 \pm 1.6) \quad (25)$$

$$R = 0.87, \sigma = 0.26$$

*Spectral ratios*

$$\lg \Delta\sigma = (0.4 \pm 0.1) \lg M_0 - (4.3 \pm 1.6) \quad (26)$$

$$R = 0.64, \sigma = 0.48$$

Zone C:

*Spectral inversion*

$$\lg \Delta\sigma = (0.7 \pm 0.1) \lg M_0 - (9.4 \pm 0.7) \quad (27)$$

*Spectral ratios*

$$\lg \Delta\sigma = (0.4 \pm 0.1) \lg M_0 - (5.0 \pm 1.0) \tag{28}$$

$$R = 0.82, \sigma = 0.40$$

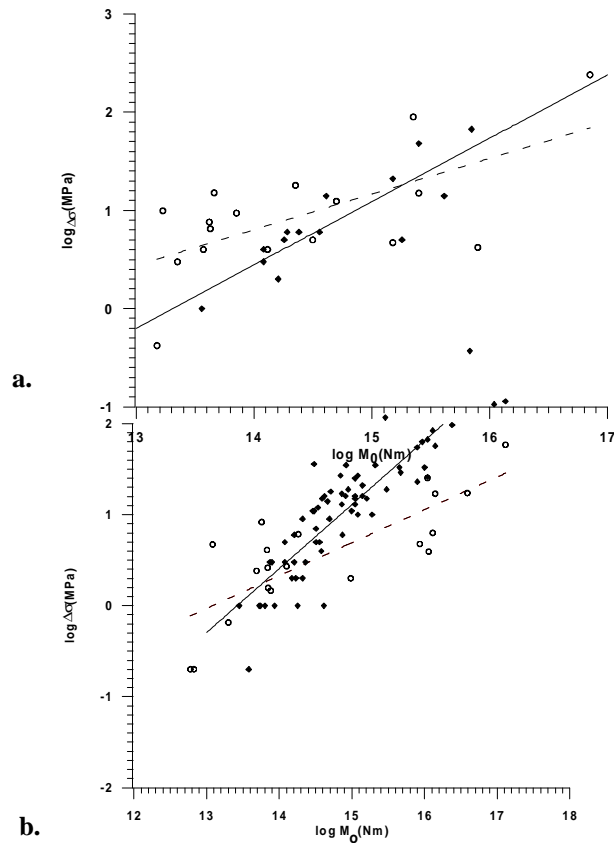


Fig. 13. - Stress drop – seismic moment relation diamonds and solid line for spectral inversion and empty circles and dashed line for spectral ratios

- a. Zone A;
- b. Zone C.

As regards the dependence of stress drop on seismic moment, this is better constraint when the spectral inversion is applied. Anyway, in all cases the slope is significantly larger than zero, (characteristic for constant stress drop scaling), indicating inhomogeneous rupture processes in the source for both segments of the subducting lithosphere.

**The relation between seismic energy and seismic moment** estimated by spectral inversion method is given by (Fig. 14):

Zone A:

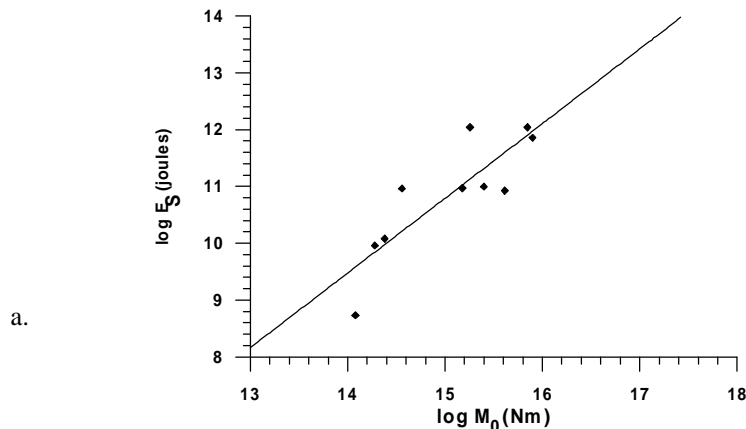
$$\lg E_s = (1.3 \pm 0.3) \lg M_0 - (9.0 \pm 4.4) \tag{29}$$

$$R=0.85, \sigma=0.60$$

Zone C:

$$\lg E_s = (1.8 \pm 0.1) \lg M_0 - (15.9 \pm 1.1) \tag{30}$$

$$R=0.95, \sigma=0.50$$



Seismic source properties

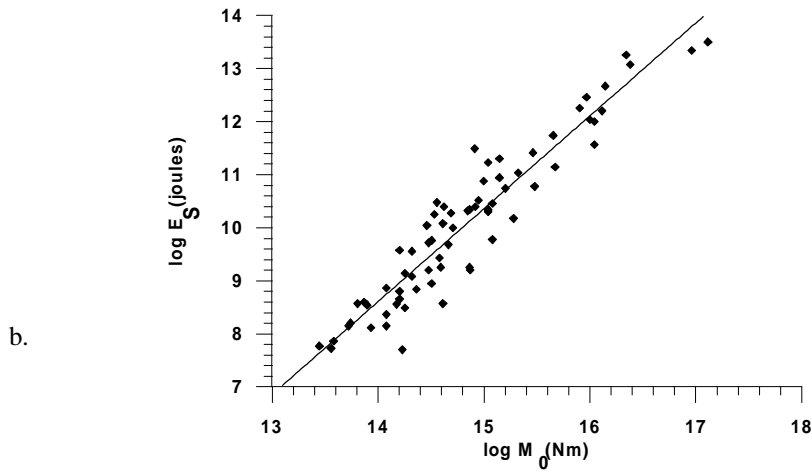


Fig. 14.- Seismic energy versus seismic moment for:  
 a. Zone A;  
 b. Zone C.

Note that concerning this type of relation, the data for A segment are insufficient to constrain the  $\log E_s \sim \log M_0$  relationship.

The relation between moment magnitude,  $M_W$  and duration magnitude,  $M_D$  is given by (Fig. 15):

Zone A:  

$$M_W = (0.8 \pm 0.3) M_D + (0.3 \pm 0.3) \quad (31)$$

$$R = 0.75, \sigma = 0.31$$

Zone C:  

$$M_W = (1.0 \pm 0.0) M_D - (1.0 \pm 0.3) \quad (32)$$

$$R = 0.91, \sigma = 0.22$$

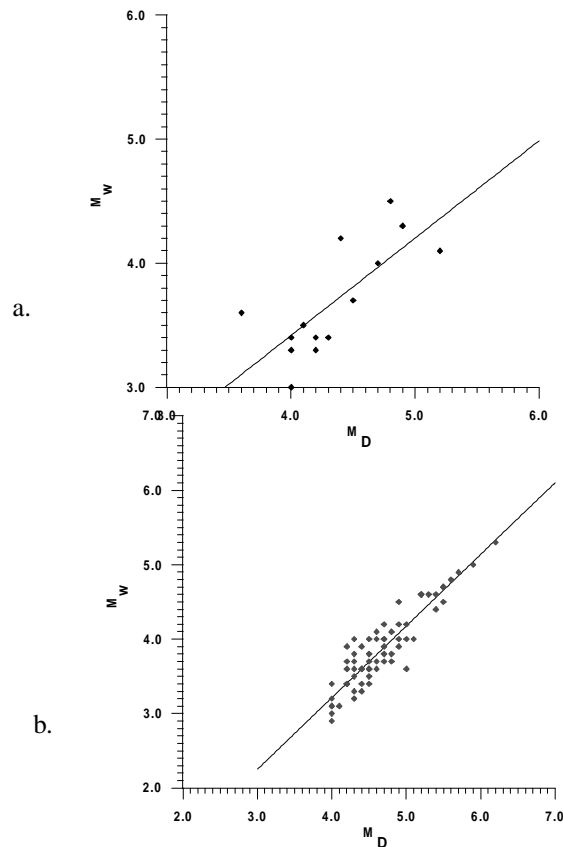


Fig. 15. -  $M_W$ -  $M_D$  relation

- a. Zone A;  
b. Zone C.

**Dislocation vs. seismic moment** is plotted in Fig. 16. The linear regression approximation computed for the spectral inversion case is:

Zone A:

$$\lg D = (0.7 \pm 0.1) \lg M_o - (10.2 \pm 1.0) \quad (33)$$

$$R = 0.95, \sigma = 0.17$$

Zone C:

$$\lg D = (0.7 \pm 0.1) \lg M_o - (10.0 \pm 0.6) \quad (34)$$

$$R = 0.92, \sigma = 0.25$$

As can be seen in the figure, the regression is well constraint with similar parameters in the two active segments.

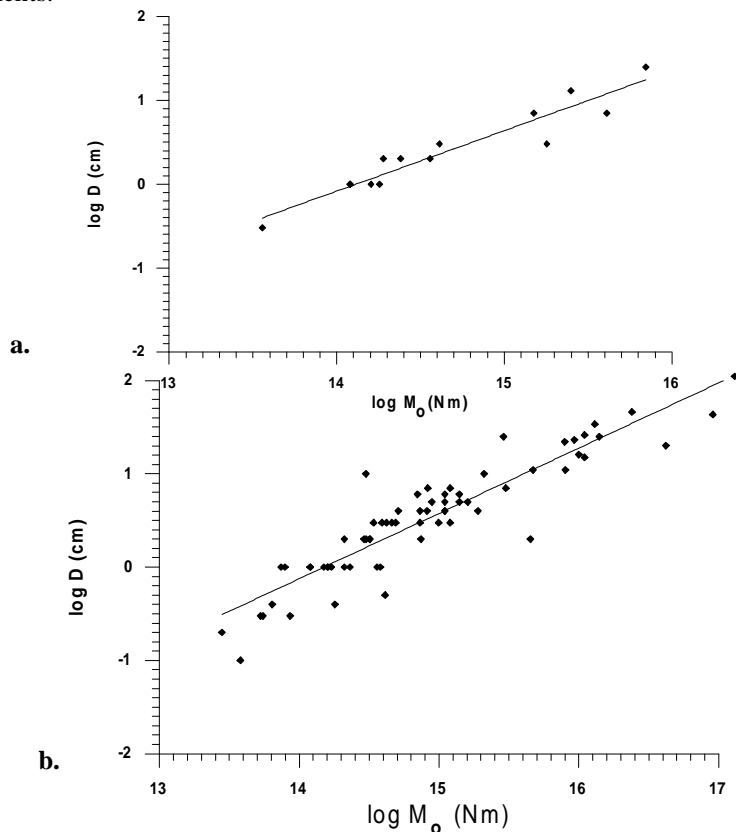


Fig. 16. - Dislocation vs. seismic moment.

- a. zone A;  
b. zone C.

## CONCLUSIONS

An extended set of earthquake data is considered to analyze the seismic source properties in the Vrancea subducting lithosphere and to detect possible depth dependence of these properties. The set consists of 100 earthquakes occurred between 1996 and 2001 with magnitudes  $M_w$  between 2.9 and 5.3. The considered time interval corresponds to the installation in Romania of a high-quality digital accelerometer network in the framework of the German-Romania CRC461 Programme [5] and to the deployment of a temporary seismic tomography experiment (CALIXTO'99 - [24]) during six months in 1999. In addition to the routine data coming from the Romanian national network (18 short-period, one-component

instruments) dedicated firstly to seismicity monitoring, the new data offers an excellent basis for advanced seismicity and seismic source research.

To constrain the source parameters we apply two independent techniques: the inversion of the P-wave displacement spectra (SRCPLUS algorithm – [20], and the spectral ratios method (applied to P-wave seismograms, as well). The application of two independent methods to common events gives us the opportunity to have an idea about the resolution of the resulted source parameters and scaling. In the case of spectra inversion we have to correct first the waveforms for instrument, radiation pattern and path effects. These corrections are not necessary in the case of spectral ratios since we can suppose that the ratios efficiently remove the corrections if the pairs of co-located earthquakes are carefully selected. The comparison between the source parameters retrieved by the two methods shows an underestimation of the source radius by spectra inversion, probably due to an incomplete correction in this case (*Fig. 3*). This implies an overestimation of the corresponding stress drop values, according to equation (4). The considering of a appropriate site effect correction will certainly reduce these discrepancies.

To account for the structural inhomogeneity in the subducting lithosphere beneath Vrancea, we separate the analysis on two segments: the upper part A ( $60 \leq h \leq 110$  km) and the lower part C ( $110 < h \leq 220$  km). A transition zone around 100 km depth seems to play an important role in the distribution of tectonic stress. Seismicity rate is lower here and the reverse faulting mechanism, which is predominant all along Vrancea subcrustal region, is changing here into normal faulting [4]. The rough two-blocks analysis on depth proposed in this paper, as a first attempt to determine the depth variation properties in Vrancea seismogenic zone, outlines important differences in the seismic moment – magnitude distribution, the seismic energy-seismic moment and the seismic energy – magnitude distribution. On the contrary, the scaling of the stress drop and dislocation with the seismic moment shows practically no depth dependence. Considering the dispersion of data, we can assume that the seismic moment – source radius distribution is also not changing on depth.

As an interesting result we outline the relations like  $\log E_s \sim \log M_0$ , approximated by least mean square method which show an apparent mean stress (the slope of the relation)  $\sigma_{app}$  from 1.3 MPa in upper segment, 1.75 in lower segment and 1.73 on the entire depth domain.

The increase of the mean apparent stress on depth agrees with the scaling relations obtained by [15] using source time function duration. The authors found that the source durations appear to decrease in the deeper part of Vrancea slab and they interpreted this result as a sign of increasing the stress drop there. This interpretation correlates well with the decrease of the slope of the frequency-magnitude distribution in the lowest part of the slab, since as it is known the b slope reflects differences in the stress regime or in the inhomogeneity distribution. However, it is still unclear if the decrease of source duration with depth reflects changes in stress drop or elastic parameters [23], [8]. Our study gives not a definitive answer to this question, which remains a subject for future research.

Fractal statistics showed at its turn the existence of significant variations on depth of the clustering properties. Thus, the analysis of the variation coefficient  $C_v$  or  $\gamma$  parameter outlined differences in the generation process of moderate-magnitude (asperity-like) events and small-magnitude (crack-like) events in the lower and upper segments of the subducting lithosphere [16]. These differences seem to reveal significant variations in the underlying physical process responsible for earthquake triggering and could bear some relation with the fluid behavior at depth. Our results partly support these hypotheses, but at this stage they cannot be conclusive, if we take into consideration the complexity of the problem.

*Acknowledgements.* Our study benefited from data recorded by the K2 network installed within the joint German-Romanian research programme CRC461 [4], [5] and the CALIXTO'99 tomography experiment [25].

## REFERENCES

1. D.J. Andrews, 1986. Objective determination of source parameters and similarity of earthquakes of different size. Proc. 5<sup>th</sup> Maurice Ewing Symp. Earthquake Source Mechanics, S. Das, J. Boatwright, and C. H. Scholtz, Editors, American Geophysical Union, Washington D.C., 259-267.
2. O. Bazacliu and M. Radulian. Seismicity variations in depth and time in the Vrancea (Romania) subcrustal region, *Natural Hazards*, 19, 165-177 (1999).
3. J. Boatwright. A spectral theory for circular seismic sources; simple estimates of source dimension, dynamic stress drop, and radiated seismic energy. *Bull. Seism. Soc. Am.*, 70, 1, 1-27 (1980).
4. K. P. Bonjer and Rizescu, M., 2000. Data Release 1996-1999 of the Vrancea K2 Seismic Network. Six CD's with evt-files and KMI v1-, v2-, v3-files. Karlsruhe-Bucharest, July 15, 2000.
5. K. P. Bonjer, Oncescu, M. C., Driad, L., Rizescu, M. (1999). A note on empirical site response in Bucharest (in Vrancea Earthquakes, Tectonics, Hazard and Risk Mitigation, Wenzel et al., eds.), p. 149-162, Kluwer Academic Publishers.
6. K. P. Bonjer, Rizescu, M. and Grecu, B., 2002. Data Release 2000-2001 of the Vrancea K2 Seismic Network. Two CD's (evt-files). Bucharest- Karlsruhe, October 24, 2002.
7. J. N. Brune. Tectonic stress and the spectra of seismic shear waves from earthquakes. *J. Geophys. Res.*, 75, 4997-5009, (1970).
8. P. Campus and S. Das. Comparison of the rupture and radiation characteristics of intermediate and deep earthquakes, *Journal of Geophysical Research*, 105, 6177-6189 (2000).
9. J. E. Ebel, Bonjer, K.-P., 1990. Moment tensor inversion of small earthquakes in southwestern Germany for the fault plane solution. *Geophys. J. Int.*, 101, 133-146.
10. D. Enescu and B. D. Enescu. Seismotectonic model regarding the genesis and the occurrence of Vrancea (Romania) earthquakes, *Rom. Reports in Phys.*, 50, 97-122, (1998).
11. G. T. Lindley. Source parameters of the 23 April 1992 Joshua Tree, California earthquake, its largest foreshock and aftershocks. *Bull. Seism. Soc. Am.*, 84, 1051-1057 (1994).

12. M. C. Oncescu. Some source and medium properties of the Vrancea seismic region, Romania, *Tectonophysics*, 126, 245-258 (1986).
13. M. C. Oncescu and M. Rizescu. CONVSEIS v4.9-Conversion program package for seismological data on PCs, *IASPEI Software Shareware Library, Karlsruhe*, 82p (1998).
14. M. C. Oncescu and C.-I. Trifu. Depth variation of moment tensor principal axes in Vrancea (Romania) seismic region. *Ann. Geophys.*, 58, 149-154, (1987).
15. M. Popa and M. Radulian. Depth-dependent scaling relations of the source parameters for the Vrancea subcrustal earthquakes, *Rom. Journ. Phys.*, 46, 499-513 (2001).
16. E. Popescu, O. Bazacliu and M. Radulian. Time clustering properties of the Vrancea (Romania) subcrustal earthquakes, *Romanian Reports in Physics*, 53, 507-518 (2001).
17. E. Popescu, O. Bazacliu, M. Radulian and L. Ardeleanu. Clustering properties of the Vrancea (Romania) intermediate depth seismicity, *Studii si Cercetari de Geofizica*, 38, 41-51. (2000).
18. E. Popescu, M. Popa, M. Radulian (2003). Efficiency of the spectral ratio method to constrain the source scaling properties of the Vrancea (Romania) subcrustal earthquakes, *Rom. Journ. Physics* (2003) (in print).
19. M. Radulian and M. Popa. Scaling of the source parameters for the Vrancea intermediate depth earthquakes, *Tectonophysics*, 261, 67-81 (1996).
20. M. Rizescu. Fully automated system for archiving, processing and transmission of seismological data, *Ph.D Thesis, Bucharest, 1998* (in Romanian).
21. C. I. Trifu and M. Radulian. Asperity distribution and percolation as fundamentals of earthquake cycle. *Phys. Earth Planet. Interiors*, 58, 277-288, 1989.
22. C. I. Trifu and M. Radulian. Frequency-magnitude distribution of earthquakes in Vrancea : relevance for a discret model. *J. Geophys. Res.*, 97, 4301-4311 (1991).
23. J. E. Vidale and H. Houston. The depth dependence of earthquake duration and implications for rupture mechanisms, *Nature*, 365, 45-47, 1993.
24. F. Wenzel, Lorenz, F., Sperner, B., Oncescu, M.C., 1998. Seismotectonics of the Romanian Vrancea area. In: Wenzel, F., Lungu, D., Novak, O.(Ed.) Vrancea Earthquakes: Tectonics, Hazard and Risk Mitigation, Kluwer Academic Publishers, Dodrecht, Netherlands, 15-25.
25. F.Wenzel, M. C. Oncescu, M. Baur, F. Fiedrich. An Early Warning System for Bucharest, *Seismological Research Letters*, Vol. 70, 161-169. (1999).